Sources, Distribution, and Water Column Processes of Aliphatic and Polycyclic Aromatic Hydrocarbons in the Northwestern Black Sea Water

ARTICLE *in* ENVIRONMENTAL SCIENCE AND TECHNOLOGY · JULY 1999

Impact Factor: 5.33 · DOI: 10.1021/es9811647

3 AUTHORS, INCLUDING:

Josep María Bayona
Spanish National Research Council
320 PUBLICATIONS **9,166** CITATIONS

Sources, Distribution, and Water Column Processes of Aliphatic and Polycyclic Aromatic Hydrocarbons in the Northwestern Black Sea Water

CRISTINA MALDONADO,[†] JOSEP M. BAYONA,*[,†] AND LAURENT BODINEAU[‡]

Environmental Chemistry Department, C.I.D.−C.S.I.C., Jordi Girona 18, E-08034, Barcelona, Catalunya, Spain, and Université de Lille, Laboratory of Analytical and Marine Chemistry, CNRS, EP1750 Elico, Bâtement C8, Villeneuve d'Asq, France

Aliphatic and aromatic hydrocarbons have been determined in (28 samples) suspended particulate matter (>0.7 μm) collected at subsurficial seawater and three vertical profiles in a transect from the continental shelf, slope, and deep basin (15 samples) of the western Black Sea. The dissolved phase (<0.7 μm) was collected at subsurficial and in the redoxcline (6 subsurficial and 5 deeper). The highest concentrations of hydrocarbons were detected in the Danube, Dnieper, and Dniester River Estuaries and other point sources of pollution located offshore Romania and Bulgaria where oil production and refining is carried out (i.e., Constantza, Varna). Concentrations of hydrocarbons decreased with increasing distance from the coast, but relatively high concentrations were found at the open stations where the particulate organic carbon (POC) is higher. Fossil PAHs are predominant in the coastal stations, and the unresolved complex mixture (UCM) of aliphatic hydrocarbons is predominantly of a fossil common origin according to the hopane and sterane distribution. The fossil to pyrolytic PAH ratio decreases with source distance attributable to a deposition of pyrolytic PAHs. The spatial distribution of PAHs found in the dissolved phase is evenly distributed. The unresolved complex mixture/alkane ratio is higher in the dissolved phase and can be attributable to a faster degradation of labile *n*-alkanes in this phase. Vertical profiles of hydrocarbons in suspended particles show two submaxima located in the biomass maximum abundance and at the redoxcline where there is an enrichment referred to POC due to phytoplankton or bacteria uptake, respectively.

Introduction

Contamination of continental seas has increased worldwide over the past decades (*1*). In the Black Sea, petroleum inputs are significant as a consequence of river discharges, accidental crude oil spills, ballast operations, sewage disposal, offshore production, and transport (*2*). Particularly, the western part of the Black Sea is receiving a number of land-based sources of pollution (i.e., Danube, Dnieper, and Dniester Rivers) being the area most affected by eutrophication, anoxia, and strong changes in the ecosystems (*3*).

Among the crude oil components, polycyclic aromatic hydrocarbons (PAHs) are of great concern since some components are mutagenic or carcinogenic (*4*). PAHs have been found ubiquitous constituents in the Black Sea sediments (*5*), but there is a lack of data on their distribution and processes occurring in the Black Sea water column. Furthermore, the oxic−anoxic zones of the Black Sea water column deserves a great interest to investigate the processes affecting the fate of hydrocarbons since it contains a large biomass of bacteria. Once hydrocarbons reach the anoxic part of the water column, it is expected to lower degradation rates in comparison with the oxic part of the water column. In this regard, the large portion of anoxic conditions (low oxygenated waters) in the water column of the Black Sea environment (*6*) offers a unique opportunity to investigate the biogeochemical processes of hydrocarbons during sedimentation. Until now, a large part of the information is focused on the biogeochemical processes occurring in suspended or sinking particles through the oxic water column (*7*−*9*). It is known that sulfate-reducing bacteria can utilize aliphatic and aromatic hydrocarbons (*10*) and that three- and four-ring PAHs are biodegradable under strict anaerobic conditions (*11*).

The aim of this paper is to re-address the lack of data on PAHs in the water column of the Black Sea in the framework of the European River Ocean Systems (EROS 2000) project focusing on the following objectives: (i) to recognize the sources and distribution of aliphatic and aromatic hydrocarbons in the dissolved phase (DP) and the suspended particulate matter (SPM) in subsurficial seawater; (ii) to investigate the fate and transformations affecting PAHs in the water column, especially those occurring in the redoxcline (boundary oxic−anoxic) and the anoxic waters of the Black Sea basin.

Materials and Methods

Environmental Setting. The Black Sea represents the largest anoxic reservoir worldwide with an area of 4.23×10^5 km^2, a volume of 5.37×10^5 km^3, and a maximum depth of 2212 m. It is connected with the eastern Mediterranean Sea through the Bosphorus Strait, which is the only link to the open ocean. The Black Sea receives freshwater from the Danube, Dniester, and Dnieper Rivers. The Danube River, with a drainage basin of 2.4×10^6 km^2 (*3*), collects the waste products of 18 European countries (ca. 160 million habitants) and is the main river discharging into the area (203 km^3 yr^{-1}) representing 77% of the total freshwater discharge into the Black Sea. Chilia, Sulina, and St.Georges are the three main Danube branches. The Chilia branch is the most important one representing 60% of the Danube discharge. The Dnieper River is outflowing northwest of the Crimean Peninsula. In the past decades, the Dnieper River has suffered man-made transformations including six shallow dams. The Dniester River belongs to Ukrania and Moldavia, forms a wide estuary south of Odessa, and constitutes an important waterway (Figure 1).

In the last three decades, an increasing nutrient supply from the riparian regions and the Danube basin has resulted in higher productivity rates of phytoplankton in the upper

* Corresponding author telephone: 34-93-4006100; fax: 34-93-2045904; e-mail: jbtqam@cid.csic.es.
[†] C.I.D.−C.S.I.C.
[‡] Université de Lille.

10.1021/es9811647 CCC: $18.00
Published on Web 07/03/1999

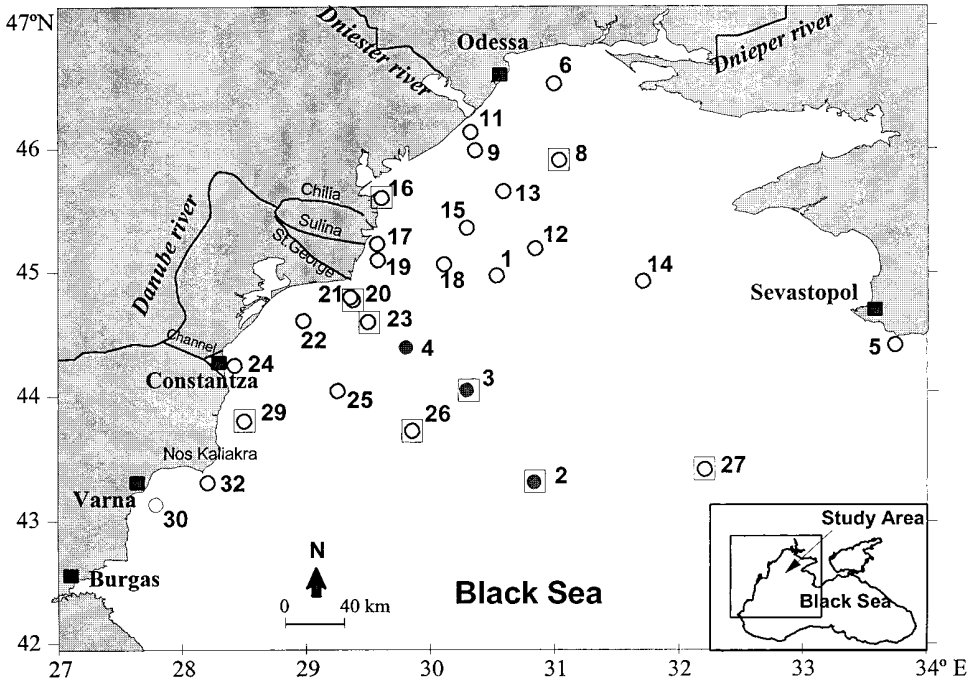

FIGURE 1. Map of the sampling area showing the stations and the kind of sample: particulate (○), dissolved (■), and vertical profile (●).

part of the water column of the Black Sea (*12*). Furthermore, river management by the construction of the two Iron Gate Dams in the drainage areas has reduced drastically water and sediment discharges, contributing to the alteration of the hydrological balance of the Black Sea and producing an alarming decrease in the depth of the pycnocline/chemocline (*6*, *13*, *14*).

The northwestern part of the Black Sea is the region most severely affected. It is a shallow semi-enclosed area with a surface area of 63.9×10^3 km^2. Romania, Bulgaria, and the European portion of Turkey border it to the west. Hydrology of the area shows a cyclonic circulation with a southward prevalent current that enhances the transport of the Danube waters toward the Romanian coastal line (*15*).

Offshore oil production, pipeline transport, and shipping are known to be important sources of oil contamination in the northwestern Black Sea (*2*). The principal harbors northwest of the Black Sea are Odessa and Sevastopol in Ukraine, Varna and Burgas in Bulgaria, and Constanza in Romania. The Constantza Harbor is the largest harbor of the Black Sea and receives more than 50% of the petroleum of the country. The Danube−Black Sea Canal has two mouths, one in the southern part and the other one 20 km north of the Constantza Harbor. In addition, petroleum from the Arabian countries and from the Black Sea itself is refined in northern Constanza (Romania) and in Bulgarian refineries. Pipeline oil transport is carried out from the offshore oil fields; one of them located 40 km offshore Constantza.

Sampling and Strategy. Temperature, salinity, fluorescence, and oxygen were obtained for whole sampling area by using a CTD Hydrocast Mark-III equipped with Go-Flo rosette bottles. Suspended particles were collected in situ during the leg II of the R/V *Professor Vodianitsky* cruise on August 1995 by filtration with stand-alone pumps (Mark II, Challenger Oceanics, U.K.). From 200 to 400 L of seawater was filtered at depths ranging from 3 to 1500 m in situ at a flow rate of 500 L h^{-1} using kiln-fired (450 °C overnight) GF/F filters (Whatman, Kent, U.K.) of 293 mm diameter and 0.7 μm of pore size. Recovered filters were folded, wrapped with precleaned aluminum foil, and stored in PTFE bags at −20 °C until they were processed in the laboratory. Subsamples of 1 L from Niskin bottles were filtered through Whatman GF/F 47 mm diameter filters to measure bulk parameters (SPM, POC, PON). Dissolved hydrocarbons were sampled from 40 L of seawater into a PTFE column packed with 50 g of XAD-2 filtered previously through 0.7 μm GF/F filters by using an in situ filtration system at depths ranging from 8 to 200 m (Infiltrex, Axys Environmental Systems Ltd, Sydney, Canada). Detailed procedures are reported elsewhere (*16*). The sampling strategy was focused on the interaction of the Danube River and the northwestern Black Sea. Accordingly, a total of 28 subsurficial particulate and 11 (subsurficial + deep) dissolved samples were collected in the northwestern part of the Black Sea (Figure 1). The Danube River prodelta, the continental shelf under the influence of the southward drift of Danube outflow, the Dniester and the Dnieper River mouth proximities, and a transect toward the open sea were collected in order to identify the sources, transport, and fate of PAHs and UCMs in the northwestern Black Sea waters and to evaluate their distribution according to the southward prevalent current in this area during the EROS-2000 Black Sea cruise leg II in August 1995 (*15*). The station (no. 5 in Figure 1) was collected at southeast Sevastopol, far from riverine inputs and not influenced by the city pollution according to the hydrographic regime. In addition, three vertical profiles of seawater particles were collected to evaluate the processes along the water column, in particular those affecting the oxic−anoxic interface where the preservation of the organic matter might play an important role in the distribution and fate of hydrocarbons in this area.

Analytical Procedures. *Elemental Analysis.* Particulate organic carbon (POC) and nitrogen (PON) were measured by dry combustion of glass fiber filters in an elemental analyzer (LECO CHNS 932, St. Louis, MO). After being dried and weighed, filters were placed in a desiccator filled with HCl fumes in order to destroy any carbonate or hydrogenocarbonate salts present in the samples. Thus, filters were dried at 60 °C, packed in a square tin foil, and injected in an induction furnace, and the evolved CO_2 and N_2 were quantitatively measured by nondispersive infrared and

TABLE 1. Bulk Parameters in Subsurficial SPM According to the Area (Mean Values in Parentheses)

sampling sites[a]	SPM (mg L^{-1})	POC (μg L^{-1})	PON (μg L^{-1})	C/N
Danube Estuary	7.0−20.5	340−1070	32.1−143	6.9−12.3
(stations 16−23)	(14.0)	(720)	(93.1)	(9.4)
Dniester & Dnieper Estuaries and Odessa depression	6.4−10.9	159−643	27.7−97.1	6.7−9.8
(stations 6, 8, 9, 11)	(9.2)	(469)	(65.6)	(8.1)
point sources pollution				
offshore Constantza	3.8−9.6	148−418	23.7−77.1	6.3−7.3
(stations 24, 25, 29)	(6.7)	(299)	(51.2)	(7.3)
offshore Varna	6.6	187	29.8	7.3
(station 30)				
offshore Nos Kaliakra	6.6	255	42.8	6.9
(station 32)				
continental shelf & slope	4.6−9.6	11−369	19.5−56.2	6.2−8.6
(stations 1, 4, 12−15, 26, 3)	(6.3)	(233)	(38.4)	(7.1)
open sea	4.8−7.7	191−225	30.4−41.0	6.4−7.4
(stations 2, 27)	(6.3)	(208)	(35.7)	(6.9)
reference	4.6	110	15.5	8.3
(station 5)				

[a] Sampling site location is indicated in Figure 1.

TABLE 2. Spatial Distribution of Aliphatic and Aromatic Hydrocarbons in Subsurficial SPM (Mean Values in Parentheses)

sampling site[a]	alkanes (ng L^{-1})	UCM (ng L^{-1})	PAHs (pg L^{-1})
Danube Estuary	11.8−125	28.2−931	477−5612
(stations 16− 23)	(62.9)	(224)	(1596)
Dniester & Dnieper Estuaries and Odessa depression	6.1−39.3	39.4−537	104−5521
(stations 6, 8, 9, 11)	(21.6)	(201)	(1609)
point pollution sources			
offshore Constantza	12.5−188	241−948	116−903
(stations 24, 25, 29)	(100)	(595)	(401)
offshore Varna	10.7	252	377
(station 30)			
offshore Nos Kaliakra	48.7	366	2219
(st 32)			
continental shelf & slope	5.4−67.3	22.0−237	132−880
(stations 1, 4, 12−15, 26, 3)	(21.6)	(105)	(394)
open sea	3.0−101	12.1−742	106−1036
(stations 2, 27)	(52)	(377)	(571)
reference	1.61	21.02	45.0
(station 5)			

[a] Sampling site location is indicated in Figure 1.

thermal conductivity cells following a calibration with organic standard compounds (i.e., sulfamethazine, caffeine).

Hydrocarbon Analysis. Collected filters were freeze-dried and spiked with the analyte surrogates, 5α-cholestane for aliphatic hydrocarbons and perdeuterated pyrene and benzo-[*ghi*]perylene for PAHs**.** Analytical procedures have been reported elsewhere (*16*). Briefly, the suspended particulate matter (SPM) extraction was performed by sonication (3 times) with 20 mL of dichloromethane−methanol (2:1) followed by centrifugation. DP was recovered from the XAD-2 columns by eluting sequentially with methanol and dichloromethane. Methanolic fraction was liquid−liquid extracted with *n*-hexane. Organic extracts were fractionated by alumina adsorption chromatography. Aliphatic hydrocarbons (fraction 1) and PAHs (fraction 2) were analyzed by GC-FID (Fisons 5000 Mega series, Milan, Italy) and GC−MS (Fisons, MD-800), respectively. PAH analyses were performed in the selected ion monitoring using a time window-scheduled acquisition with the diagnostic ions at *m*/*z* 166, 178, 184, 188, 192, 198, 202, 212, 206, 212, 228, 252, 276, 278, and 288. Hopanes and steranes were determined by GC−MS by using the *m*/*z* 191 and 217 as diagnostic ions, respectively.

Quantitation. The internal standard (IS) procedure was used for quantitation, 5α-androstane was used as the IS for aliphatics, and perdeuterated anthracene was used as the IS for aromatics. Quantitation of *n*-alkanes was based on an external calibration mixture containing *n*-C_{14}, *n*-C_{15}, *n*-C_{16}, pristane, *n*-C_{22}, *n*-C_{23}, *n*-C_{24}, *n*-C_{28}, *n*-C_{32}, and *n*-C_{36} according to the response factor of the closest eluting compound. On the other hand, the response factor applied to the UCM quantitation was the external standard eluted in its maximum abundance. The calibration mixture for PAH quantitation contained analyte surrogates spiked in the sample and 14 PAHs included in the U.S. EPA priority pollutants list. Recoveries of spiked filters according to the standard addition procedure were higher than 80%, and the RSDs were below 15% ($n = 3$). Procedural blanks and control samples were processed in the same manner as real samples, and they were below 5% of the analyte abundance of analytes. Quantitative data were corrected for recovery.

Statistics. Multiple regression analyses were performed using the multivariate data analysis software Pirouette (Infometrix, WA). The confidence level was 95% ($p < 0.05$). To prevent misinterpretations due to the large values of some of the variables, data were standardized (i.e., zero mean and unit variance).

Results and Discussion

Spatial Distribution of the Organic Matter and Hydrocarbons. *Bulk Parameters.* Concentrations of the SPM in the subsurficial waters of the western Black Sea ranged between 3.8 and 20.5 mg L^{-1} (Table 1). SPM concentrations showed

TABLE 3. Normalized Distribution of Aliphatic and Aromatic Hydrocarbons in Surficial SPM According to the POC Content (Mean Values in Parentheses)

sampling sites[a]	alkanes (μg g^{-1} POC)	UCM (μg g^{-1} POC)	PAHs (ng g^{-1} POC)
Danube Estuary	11−261	26−1115	0.4−10.3
(stations 16−23)	(90)	(540)	(2.7)
Dniester & Dnieper Estuaries and Odessa depression	34−38	96−390	0.2−2.2
(stations 6, 8, 9, 11)	(30)	(230)	(1.1)
point pollution sources			
offshore Constantza	84−567	1627−2870	0.4−2.7
(stations 24, 25, 29)	(330)	(2250)	(1.3)
offshore Varna	57	1344	2.0
(station 30)			
offshore Nos Kaliakra	191	1436	8.7
(station 32)			
continental shelf & slope	22−201	60−1138	0.4−6.3
(stations 1, 4, 12−15, 26, 3)	(100)	(530)	(2.4)
open sea	16−449	64−3299	0.6−4.9
(stations 2, 27)	(232)	(1680)	(2.8)
reference	15	191	0.4
(station 5)			

[a] Sampling site location is indicated in Figure 1.

TABLE 4. Reported Values of Aromatic Hydrocarbons in the SPM and the DP (pg L^{-1}) (Mean Values in Parentheses)

	total PAHs		parent PAHs		
zone	SPM	DP	SPM	DP	references
Seawater					
Aegean Sea (Eastern Mediterranean)	395−1239 (756)	383−1354 (653)	80.5−303 (177)	113−489 (216)	Gougou[a]
Western Mediterranean continental shelf	305−772 (525)	na[b]	na	na	9
Western Mediterranean open sea	203−605 (370)	710	na	na	9
Baltic Sea	na	na	49−258 (193)	300−594 (526)	20
Northwestern Black Sea shelf & slope	132−880 (394)	952	52.6−269 (137)	471	this study
Freshwater and Estuaries					
Danube Estuary	477−5612 (1596)	287−422 (355)	130−1253 (442)	183-214 (199)	this study
Dnieper & Dniester Estuaries	104−5521 (1609)	183	42.9−1397 (467)	106	this study
Chesapeake Bay Estuaries	na	na	1826−23376 (8330)	3236−43206 (14710)	22
Lake Superior	na	na	752	na	23
Ebro Estuary	566	2170	na	na	9

[a] Personal communication. [b] na, not available.

a spatial variability, and two separate areas could be distinguished. The first set of stations is located close the northwestern coast where the highest SPM loads, up to 20 mg L^{-1}, were registered. It is attributable to land-derived inputs via Danube and other minor rivers (i.e., Dniester, Dnieper) and also to sediment resuspension in the shallow waters. The SPM concentrations of the second group of stations located in the continental shelf and slope of the Black Sea were quite similar (from 3.8 to 7.7 mg L^{-1}, average: 5.1 mg L^{-1}).

In general, the spatial distributions of POC and of PON follow closely that of the SPM. POC values ranged from 11 to 1070 mg L^{-1} (Table 1) and correlated well with the concentrations of SPM ($N = 25$, $r^2 = 0.95$, $p < 0.01$). As for SPM, POC was spatially distributed into two distinct zones. In the former, highest values (from 159 to 1070 μg L^{-1}) have been found close to the northwestern coasts while lowest POC concentrations (<370 μg L^{-1}) were observed in the offshore waters. The atomic C/N ratio is higher in river estuaries (C/N = 8.1−9.4) and slightly lower in the rest of the stations (C/N = 6.9−7.3) (Table 1), which is consistent with a predominance of planktonic organic matter and a moderate input of terrestrial organic matter in the river influenced areas. The average C/N atomic ratio of 9 of the whole sampling set falls within the range of 8−10 typically reported for world rivers by Meybeck (*17*).

TABLE 5. Distribution of Dissolved Aliphatic and Aromatic Hydrocarbons in Subsurficial Water (Mean Values in Parentheses)

sampling sites	alkanes (ng L^{-1})	UCM (ng L^{-1})	PAHs (pg L^{-1})
Danube Estuary	24.1−49.6	609−760	287−422
(stations 20, 23)	(36.7)	(685)	(355)
Odessa depression	24.1	609	183
(station 8)			
offshore Constantza	21.4	222	455
(station 29)			
slope	25.6	932	952
(station 26)			
open sea	11.9	221	108
(station 27)			

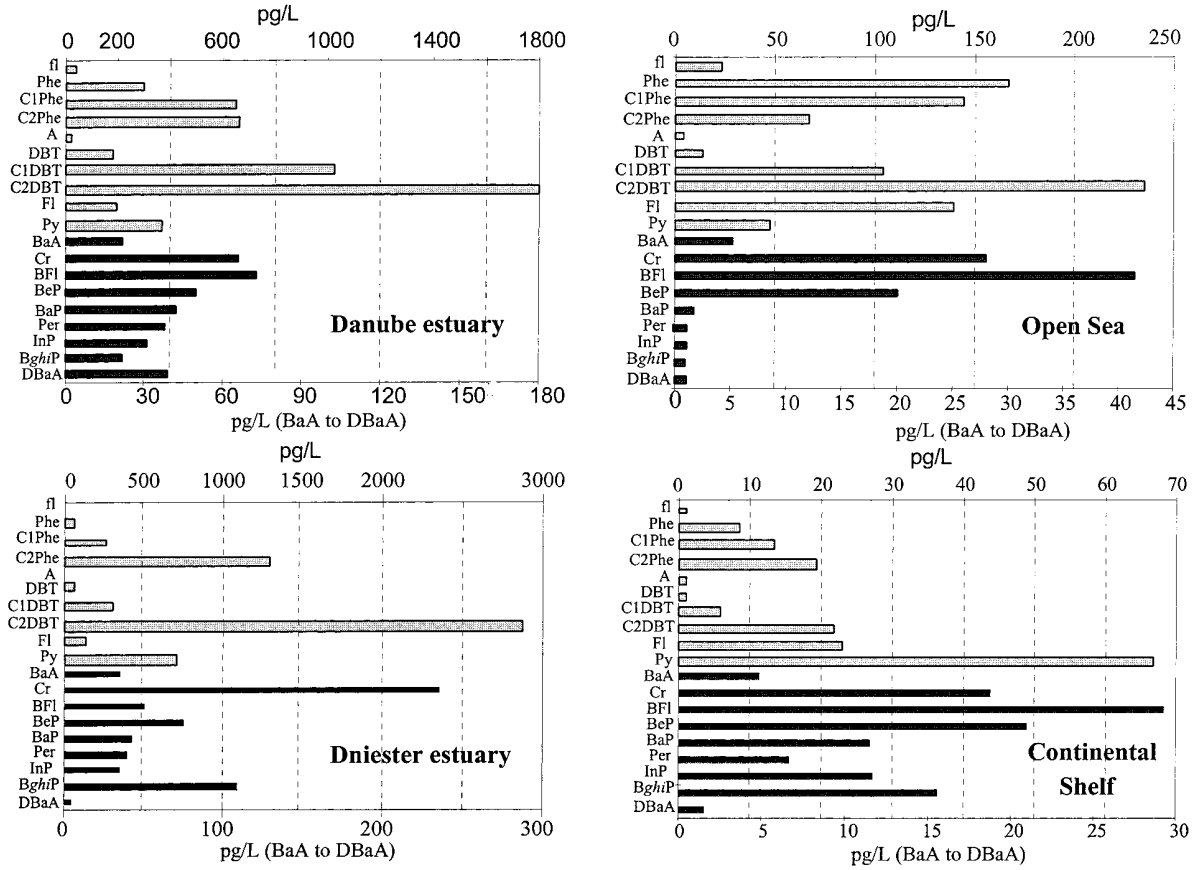

FIGURE 2. Distribution patterns of individual PAHs in the SPM according to the area of study: Danube Estuary (station 20), Dniester Estuary (station 11), open sea (station 27), and continental shelf (station 12). Locations are shown in Figure 1. Compound identification as follows: fl, fluorene; Phe, phenanthrene; C1/C2-Phe, methyl and dimethylphenanthrenes; A, anthracene; DBT, dibenzothiophene; C1/C2DBT, methyl and dimethyldibenzothiophenes; Fl, fluoranthene; Py, pyrene; BaA, benz[*a*]anthracene; Cr, chrysene; BFl, benzofluoranthenes; BeP, benzo-[*e*]pyrene; B[*a*]P, benzo[*a*]pyrene; Per, perylene; InP, indeno[1,2,3-*cd*]pyrene; B[*ghi*]P, benzo[*ghi*]perylene; DBaA, dibenz[*ah*]anthracene. Concentrations of fluorene to pyrene are given on the top axis whereas benz[*a*]anthracene to dibenz[*a,h*]anthracene are given on the bottom axis.

PAH and Aliphatic Hydrocarbons in the SPM. Subsurface concentrations of PAHs in the SPM according to the sampling area are summarized in Table 2. The highest concentrations of PAHs are found at the Danube (477−5612 pg L^{-1}) and at the Dnieper and Dniester (104−5521 pg L^{-1}) Estuaries. Other point pollution sources have been identified offshore Constantza (116−903 pg L^{-1}) and the Bulgarian coast (2219 pg L^{-1}), which are nearly 2 orders of magnitude higher than the reference station (no. 5 in Figure 1, 45 pg L^{-1}) far from the influence of point sources of pollution. The PAH concentrations in the SPM show a decline of concentrations along the continental shelf and slope according to the coast distance. In the frontal area (station 27 in Figure 1), concentrations are higher (1036 pg L^{-1}) and can be attributable to its high POC. In fact, when the PAH concentrations are normalized to the POC, they are more evenly distributed ranging from 0.2 to 10.3 ng g^{-1} POC (Table 3).

In an attempt to correlate the subsurficial distribution of PAHs, multiple linear regression (MLR) was computed considering bulk parameters concurrently measured during the sampling campaign (i.e., temperature, salinity, fluorescence, SPM, POC, PON) as independent variables. Only 42% and 40% of total variance was explainable for total and pyrolytic PAHs (benzofluoranthenes, benzopyrene isomers, indeno[1,2,3-*cd*]pyrene, and benzo[*ghi*]perylene; *18*, *19*). However, fossil PAHs (methyl and dimethylphenanthrenes, methyl and dimethyldibenzothiophenes) were significantly correlated with POC, salinity, and PON ($R_{sq\ adj}$ = 85%). It reflects dilution processes in the estuaries and the phase association with biomass of planktonic or bacterial origin (*20*) with fossil PAHs. The lack of correlation of total PAHs and pyrolytic PAHs with the SPM concentrations can be attributable to limited capacity for particulate (soot) water desorption or exchange (*21*). In a previous study, we have found a similar trend in sinking particles collected in a productive sea (Alboran, southwestern Mediterranean) (*8*). The concentrations of PAHs in the SPM of the Danube, Dnieper, and Dniester Estuaries (ca. 1600 pg L^{-1}) are higher than in other estuaries of the western Mediterranean (Ebro, 560 pg L^{-1}) (Table 4). However, these concentrations are significantly lower than other estuaries of highly polluted rivers outflowing in the Chesapeake Bay (8330 pg L^{-1}). In the continental shelf and slope, concentrations are lower than in the western Mediterranean, but in the open sea, PAH concentrations in the western Black Sea are significantly higher. which can be attributable to a different hydrodynamic regime. Concentrations of parent PAHs in the Baltic Sea are similar to those of the western Black Sea but consistently lower than values from the Lake Superior (Table 4). Therefore, the western Black Sea can be considered as a medium PAH contaminated sea.

The PAHs in the DP were evenly distributed as compared to the SPM, and the highest PAH content was found at the continental slope (952 pg L^{-1}) followed by offshore Constantza (455 pg L^{-1}) and the Danube prodelta area (355 pg L^{-1}) (Table 5). At the open sea, PAH concentrations occurred at lower

TABLE 6. Selected Ratios in the SPM and DP According to the Sampling Area (Mean Values in Parentheses)[a]

sampling sites	UCM/Alk	CPI $_{marine}$	CPI $_{terrestrial}$	CPI $_{total}$	Pr/Ph	F/P	BeP/(BeP+BaP)	BaA/(BaA+Cr)
				SPM				
Danube delta area	0.9−7.1	1.2−16.0	0.8−2.8	1.2−12.9	0.7−5.2	2.3−10.2	0.41−0.73	0.12−0.36
(stations 16−23)	(3.8)	(4.8)	(1.6)	(4.8)	(2.0)	(6.6)	(0.59)	(0.23)
Dniester & Dnieper Estuaries and Odessa depression	4.5−13.6	5.6−2.8	0.8−5.5	5.6−12.7	1.4−1.9	1.7−12.0	0.49−0.64	0.13−0.31
(stations 6, 8, 9, 11)	(7.8)	(8.6)	(3.0)	(8.0)	(1.2)	(4.8)	(0.58)	(0.22)
point pollution sources								
offshore Constantza	5.1−9.3	3.7−14.3	0.8−1.6	2.1−14.1	0.8−2.4	1.5−7.9	0.54−0.90	0.15−0.24
(stations 24, 25, 29)	(12.2)	(9.0)	(1.2)	(8.1)	(1.6)	(4.0)	(0.68)	(0.19)
offshore Varna (station 30)	23.5	2.3	0.8	2.2	14.4	10.3	0.71	0.16
offshore Nos Kaliakra (station 32)	7.5	2.0	1.6	1.8	2.4	15.1	0.71	0.23
continental shelf & slope	1.9−25.2	1.5−16.3	0.8−3.0	1.8−13.2	0.8−10.8	0.7−5.2	0.55−0.87	0.14−0.31
(stations 1, 4, 12−15, 26, 3)	(7.1)	(8.2)	(1.8)	(7.0)	(2.6)	(4.0)	(0.67)	(0.20)
open sea	4.0−14.7	4.7−4.8	0−0.8	4.1−4.4	1.8−2.1	2.4−25.2	0.92	0.16
(stations 2, 27)	(9.3)	(4.8)	(0.4)	(4.3)	(2.0)	(13.8)		
reference (station 5)	13.1	7.1	0.8	6.4	0.1	0.7	0.79	0.22
				DP				
Danube Estuary	15.3−25.2	0.9−1.0	0.9	0.9	0.9−1.0	1.5−2.1	0.46−0.84	0.12−0.15
(stations 20, 23)	(20.3)	(0.95)			(0.95)	(1.8)	(0.61)	(0.14)
Odessa depression (station 8)	25.2	1.0	0.9	0.9	0.9	1.3	0.87	0.07
offshore Constantza (station 29)	10.4	1.5	1.4	1.5	0.7	2.9	0.67	0.07
slope (station 26)	36.4	1.98	nd	1.8	1.1	1.9	0.61	0.06
open sea (station 27)	18.6	1.0	1.7	1.4	2.6	2.6	0.62	0.22

[a] CPI $_{marine} = \sum C_{(2n+1)}/\sum C_{2n}$ ($n = 7-12$); CPI $_{terrestrial} = \sum C_{(2n+1)}/\sum C_{2n}$ ($n = 13-17$); CPI $_{total} = \sum C_{(2n+1)}/\sum C_{2n}$ ($n = 7-17$); UCM, unresolved complex mixture; Pr, pristane; Ph, phytane; F, fossil PAHs, sum of methyl- and dimethylphenantrenes, methyl- and dimethyldibenzothiophenes; P, pyrolytic PAHs, sum of anthracene, fluoranthene, benz[*a*]anthracene, benzofluoranthenes and benzopyrenes; BaP, benzo[*a*]pyrene; BeP, benzo[*e*]pyrene; BaA, benz[*a*]anthracene; Cr, chrysene.

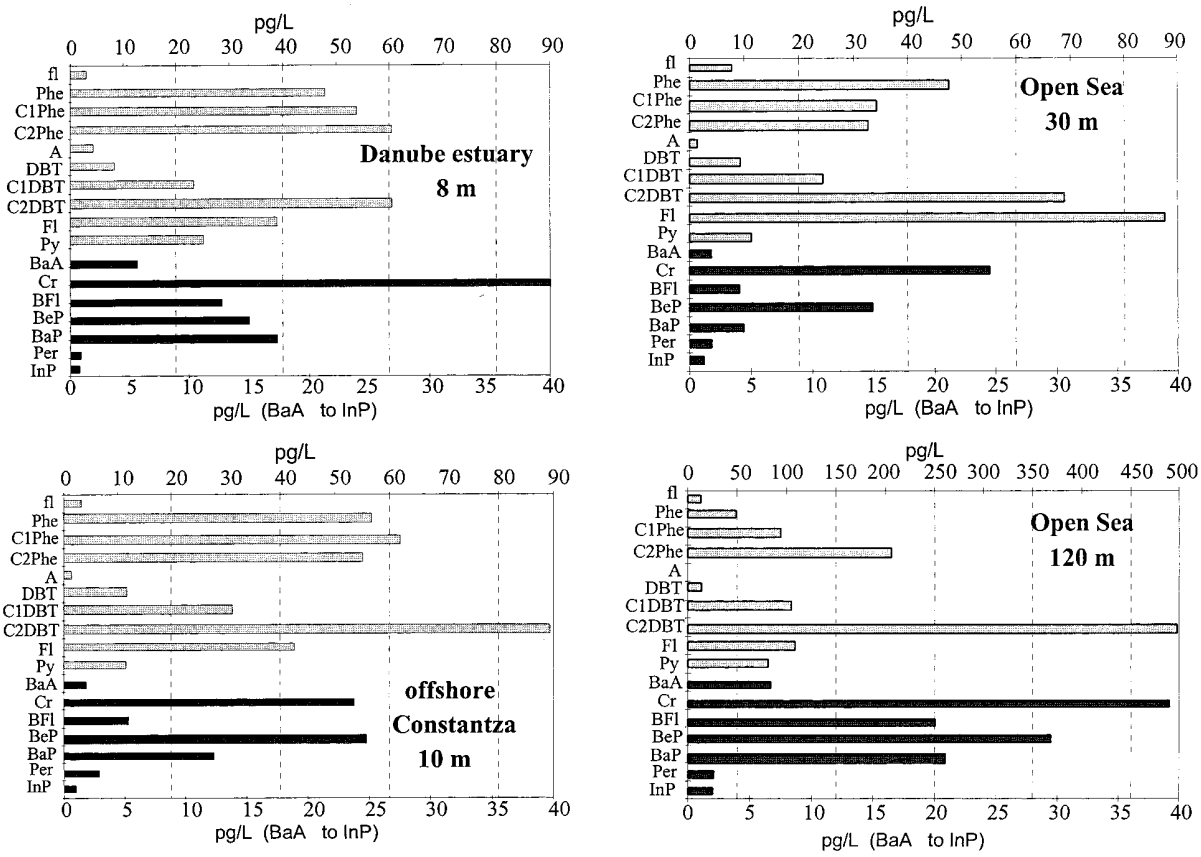

FIGURE 3. Distribution patterns of individual PAHs in the DP at open sea (station 2), at the Danube Estuary (station 20), and offshore Constantza (station 29). Compound identification is shown in the Figure 2 legend, and the sampling site location is given in Figure 1. Concentrations of fluorene to pyrene are given on the top axis whereas benz[*a*]anthracene to indeno[1,2,3-*cd*]pyrene are given on the bottom axis.

levels (108 pg L^{-1}). The concentrations of PAHs in the DP of the Danube River Estuary are lower than other rivers from the western Mediterranean (Ebro 2170 pg L^{-1}), but the concentrations found in the open western Black Sea (108−952 pg L^{-1}) are slightly higher to those concentrations found in the open eastern or western Mediterranean (113−710 pg L^{-1}) (Table 4). Concentrations of parent PAHs in the Baltic Sea (526 pg L^{-1}) are slightly higher than the western Black Sea (471 pg L^{-1}).

The UCM concentrations of aliphatic hydrocarbons in the SPM maximized at the stations collected in the river estuaries (212 ng L^{-1}) and other point sources of oil pollution such as Constantza and offshore Bulgaria (i.e., Nos Kaliakra and Varna), exhibiting concentrations even higher than river estuaries (252−595 ng L^{-1}) (Table 2). Concentrations in the continental shelf and slope declined (105 ng L^{-1}), but higher concentrations were detected in some open stations (742 ng L^{-1}) concurring with high POC concentrations attributable to the patchiness distribution of phytoplankton. In the DP, the UCM concentrations are slightly higher than in the SPM ranging from 609 to 658 ng L^{-1} in the river estuaries declining to 221 ng L^{-1} in the open sea. Similar to PAHs, the concentration of the UCM in the slope was higher than in the river estuaries.

Sources of Hydrocarbons. The PAH distributions in the SPM of estuaries and near pollution sources are characterized by a predominance of phenanthrene and the alkylated homologues of phenanthrene and dibenzothiophene among the lower molecular weight PAHs as well as chrysene at the higher molecular range (Figure 2). This PAH distribution is characteristic of fossil fuel or uncombusted fossil fuel residues (18, 19). The pattern of the alkylated species is different from

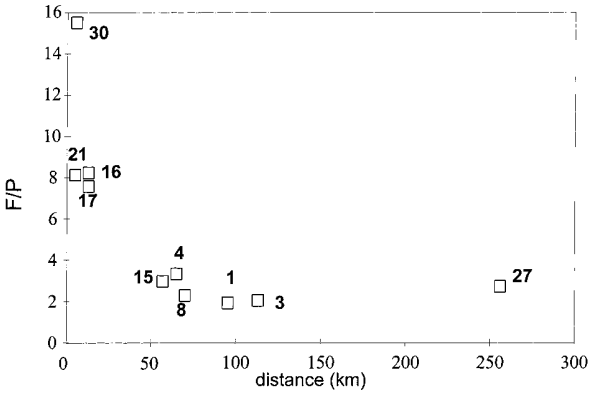

FIGURE 4. Variation of fossil/pyrolytic ratio (F/P) with the coast distance in a selected transect. The sampling site location is given in Figure 1. See Table 6 legend for fossil and pyrolytic PAHs identification.

those reported in the western Mediterranean Sea and the Chesapeake Bay (9, 24). In the western Black Sea SPM, the higher contribution of the alkylated species denotes a higher fossil input (F/P > 4, Table 6) but far from riverine inputs, pyrolytic PAHs predominates (F/P = 0.7 in Table 6).

Moreover, dimethylphenanthrenes (C_2-DMP) predominate over methylphenanthrenes (C_1-DMP) in the SPM collected in estuaries and other pollution sources contrasting with the distribution found in the Mediterranean SPM, where C_1-DMP predominates over C_2-DMP (9) attributable to higher contribution of pyrolytic sources. A similar alkylphenanthrene distribution maximized at the C_2 substitution was found in

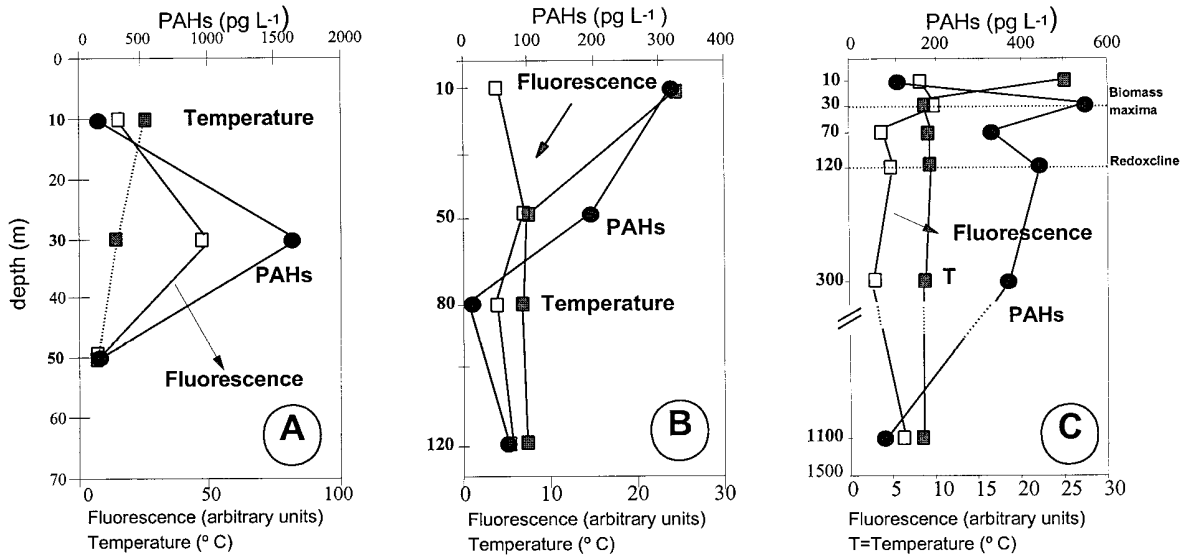

FIGURE 5. Vertical profiles of temperature, fluorescence, and PAH concentration: (A) station 4, (B) station 3, (C) station 2. The sampling site location is given in Figure 1. Concentrations of PAHs are given on the top axis whereas fluorescence and temperaure are given on the bottom axis.

the Black Sea sediments collected at the vicinities of the Danube River Estuary (5), suggesting that degradation or solubilization processes occurring during precipitation (7, 25) are less significant in the Black Sea as compared to well oxygenated water column.

The distribution found in the DP of subsurficial waters is also dominated by the alkylated dibenzothiophenes and phenanthrenes (Figure 3). However, the predominance of fossil PAHs (F/P = 0.7−2.9 in Table 6) is lower than in the particulate phase (F/P = 4.0−13.4 in Table 6). A possible explanation of that partitioning behavior is the contribution of PAHs in the colloidal form or in very fine particles (<0.7 μm), and thus they are not retained in the glass fiber filter as SPM.

Furthermore, the relatively low pristane-to-phytane ratio from 1.2 to 2.6 (Table 6) and from 0.7 to 2.6 (Table 6) in the SPM and the DP, respectively, is also suggesting a predominance of fossil hydrocarbons (26, 27). The fossil origin of the UCM was confirmed by the GC/MS identification of the 17α-(H),21β(H)-hopanes and steranes. Many of these compounds are ubiquitous in crude oils (28, 29) and, unlike many other hydrocarbons, are slightly affected by the weathering processes and bacterial degradation; therefore, their occurrence in the Black Sea samples is supporting the petrogenic origin of the UCM (30, 31). Furthermore, the similar ratios for most of the samples between 18α(H)-22,29,30-trisnorneohopane (Ts) and 17α(H)-22,29,30-trisnorhopane (Tm), the C_{29}/C_{30}, C_{32} 20S/(20S+20R), and C_{33} 20S/(20S+20R)-hopanes, being 0.50 ± 0.02, 0.95 ± 0.21, 0.71 ± 0.14, and 0.59 ± 0.07, respectively, could indicate a predominant common origin of fossil hydrocarbons in the Black Sea.

n-Alkanes in the SPM are mostly derived from algal origin evidenced with a large predominance of n-C_{17} over pristane (C_{17}/Pr = 38−186) and high CPI values for the marine n-alkanes (CPI_{marine} = 3.8−13.1) (Table 6). Interestingly, stations near the Danube Estuary exhibited a CPI characteristic of fossil hydrocarbons and the terrestrial signal was only apparent in other estuaries (i.e., Dniester).

The UCM/alkane ratio in the SPM is moderate except in stations that are chronically polluted by sewage sludges such as offshore Constantza and Varna (Table 6). The same ratio in the DP is much higher (10.4−36.4, Table 6) than in SPM, which is attributable to the easier biotic degradation processes of n-alkanes in this phase (32).

Processes during Transport. Subsurficial Processes. The fossil PAH content decreases from near-source toward the central basin of the Black Sea (F/P ratio in Table 6). Although the alkylated derivatives of phenanthrene and dibenzothiophene are the predominant compounds, there is an enrichment of pyrolytic PAHs such as benzofluoranthenes, benzopyrenes, and indeno[1,2,3-cd]pyrene (see Figure 2). This PAH distribution is comparable to those found in the western Mediterranean marine aerosols and the aerosols collected in remote areas (19, 33), suggesting an atmospheric transport and dry or wet deposition on surficial waters. The enrichment on pyrolytic PAHs according to coast distance is illustrated in Figure 4 and could be attributable to the vapor-particle partitioning of fossil PAHs and the different particle association of pyrolytic and fossil PAHs. While pyrolytic PAHs are strongly associated to fine soot particles, fossil PAHs are preferently associated to coarser particles (34). Fossil PAHs could also condense as a coating onto already-formed soot particles being more bioavailable (33). Long-range atmospheric transport of fine particles (<0.7 μm) is supported by these results. In the Black Sea, the prevalent winds over Europe would enhance aeolian transport of PAHs from industrialized eastern Europe, Russia, and northern Turkey to the central basin (5).

Another important significant feature is the decay of labile PAHs such as benzo[a]pyrene and benz[a]anthracene during the transport. In fact, a significant increase in the BeP/BeP+BaP and a moderate decrease in the BaA/Cr+BaA has been found in the area of study according to the coast distance (Table 6). The selective decay of BaA and BaP is accounted for by the higher lability of these PAHs in front of photochemical reactions which can occur during the transport (35).

Water Column Processes. Characteristic vertical PAH profiles are shown in Figure 5. The continental shelf (station 4 in Figure 5A) showed a concentration maxima of PAHs in the biomass and POC maxima (30 m) and depth-depletion profile. This vertical profile is in agreement with the introduction of contaminants into the surface waters, uptake by phytoplankton and their degradation, or desorption along the water column. A similar vertical profile was found in the western Mediterranean under well-developed thermocline (9).

In the slope, the PAH concentration maximum is found in surficial waters declining the PAH concentrations with depth (Figure 5B). A near-bottom enrichment of PAH concentration is consistent with sediment resuspension from the continental shelf and lateral transport through the submarine canyon toward the abyssal plain, which is also apparent in the POC. The strongly well-developed thermocline at this station could prevent the diffusion of PAHs to the biomass maxima located at 50 m depth.

The deep sea station (station 2 Figure 5C) presented two concentration submaxima, at the biomass (30 m depth) and at the redox boundary (120 m depth), exhibiting a depth-depletion profile. In the redoxcline, the concentration in the DP shows a significant increase in the PAH concentration accounted for mostly by the alkylated phenanthrenes and dibenzothiophenes (Figure 3). Redox boundaries are generally regions of intensified bacterial biomass and activity and also intense alteration of particulate organic matter (36). Calculations of PAH concentrations relative to POC show a maxima in the region of the oxic−anoxic boundary. At this zone, therefore, particles are significantly enriched in PAHs relative to OC. The ratio between alkylated mono- and diphenanthrenes vs. phenanthrene is minimized in the redoxcline and the biomass maxima (C_1Phe+C_2Phe/Phe = 3.60−3.67) vs. other values at different water column depths (C_1Phe+C_2Phe/ Phe = 4.13−6.70). On the other hand, the fluoranthene−pyrene ratio also reaches a minimum value at the redoxcline (Fl/Fl + Py = 0.16) vs. the other values found at other water depths (Fl/Fl+Py = 0.20−0.32). As it is well-known, the degradation kinetics of PAHs are compound-dependent, affecting to different extents the isomers or the degree of alkyl substitution (37).

Evidence of diagenetic processes occurring in the water column is also apparent in the perylene vertical profile at station 2, which is originated in the anoxic zone in the water column from different precursors (38). To the best of our knowledge, the in situ formation of perylene has only been reported in anoxic sediments (39, 40), but the formation in the oxic−anoxic interface of the Black Sea water column where a large bacterial biomass is developed could support its bacterial-mediated origin from precursors. Although terrestrial matter is the most common precursor of perylene, its formation at a remote station could evidence other origins.

At the deepest station, fossil PAHs are almost depleted as compared to pyrolytic PAHs. In this regard, the fossil-to-pyrolytic ratio is 18 times higher at the surface, evidencing desorption−degradation processes through the water column. Similar decay of fossil PAHs has been observed in the western Mediterranean where the water column is well oxygenated. However, in the Mediterranean Sea, the PAH concentration at the deepest waters are only 33% of surface values (9), but in the Black Sea, deep water concentrations account for 44% of the surficial values. The large anoxic portion of the water column in the Black Sea waters could better preserve PAHs associated to SPM along their transit through it.

Vertical profile of the UCMs shows also a submaxima at 30 and 120 m water column depths that corresponds to biomass and redoxcline, respectively. Since the ratio between UCM and POC increases at both submaxima (UCM/POC = 10.03−11.46) as compared to the other depths (UCM/POC = 0.06−4.95), it suggests that there is an enrichment.

In summary, the western Black Sea can be considered a moderately contaminated sea by hydrocarbons mostly of fossil origin coming from river inputs and other point sources of pollution. The spatial distribution of fossil PAHs in the SPM is controlled by salinity, POC, and PON. The vertical profiles of PAHs and UCMs show two submaxima at the biomass and redoxcline where the composition of PAHs is modified attributable to bacterial processes. The large portion of anoxic conditions in the water column leads to a better preservation of hydrocarbons through the water column than in well-oxygenated seas allowing a large portion of PAHs to reach the sediment.

Acknowledgments

Financial funding was obtained from the European Union (Contract EV5V-CT94-051). Sampling strategy and technical assistance in the sampling cruise was given by Dr. J. Dachs. Authors are indebted to captain and cruise personnel of the R/V Professor Vodianitsky for their friendly and positive cooperation during the sampling cruises. Technical assistance in GC and GC−MS was provided by Mrs. R. Mas, R. Chaler, and R. Alonso. Encouragement and comments given by Prof. J. Albaiges during this project are kindly acknowledged.

Literature Cited

(1) EMECS '90. Mar. Pollut. Bull. 1991, 23, 3−812.
(2) Mee, L. Ambio 1992, 21, 278−286.
(3) Leppakoski, E.; Mihnea, P. E. Ambio 1996, 25, 380−389.
(4) Polynuclear Aromatic Compounds: Part 1, Chemical, Environmental and Experimental; IARC Monographs on the Evaluation of Carcinogenic Risk of Chemicals to Humans Vol. 32; December 1983.
(5) Wakeham, S. G. Mar. Chem. 1996, 53, 187−205.
(6) Buesseler, K. O.; Livingston, H. D.; Ivanov, L.; Romanov, A. Deep-Sea Res. 1994, 283−296.
(7) Lipiatou, E.; Marty, J. C.; Saliot, A. Mar. Chem. 1993, 44, 43−44.
(8) Dachs, J.; Bayona, J. M.; Fowler, S.; Miquel, J. C.; Albaigés, J. Mar. Chem. 1996, 52, 75−86.
(9) Dachs, J.; Bayona, J. M., Raoux C.; Albaigés, J. Environ. Sci. Technol. 1997, 31, 682−688.
(10) Rueter, P.; Rabus, R.; Wilkes, H.; Aeckersberg, F.; Rainey F. A.; Jannasch, H. W.; Widdel, F. Nature 1994, 372, 455−458.
(11) McNally, D. L.; Mihelcic, J. R.; Lueking, D. R. Environ. Sci. Technol. 1998, 32, 2633−2639.
(12) Gomoiu, M.-T. In Marine Coastal Eutrophication; Marchetti, R., Viviani, R., Eds.; Elsevier: Amsterdam, 1992; p 683.
(13) Tolmazin, D. Prog. Oceanogr. 1985, 15, 217−276.
(14) Humborg, C.; Ittekkot, V.; Cociasu, A.; Bodungen, B. V. Nature 1997, 386, 385−388.
(15) Stokozov, N. A.; Polikarpov, G. G.; Shurov, S. V. Hydrodynamic interaction and water masses mixing between Danube River and the Black Sea: long-term data and EROS project results; European Commission EROS Project; ISPRA: June 11−13, 1998.
(16) Dachs, J.; Bayona, J. M. Chemosphere 1997, 35, 1669−1679.
(17) Meybeck, M. Am. J. Sci. 1982, 282, 401−450.
(18) Sporstol, S.; Gjos, N.; Lichtenthaler, R. G.; Gustavsen, K. O.; Urdal, K.; Oreld, F.; Skel, J. Environ. Sci. Technol. 1983, 17, 282−286.
(19) Sicre, M. A.; Marty, J. C.; Saliot, A.; Aparicio, X.; Grimalt, J.; Albaigés, J. Atmos. Environ. 1987, 21, 2247−2259.
(20) Broman, D.; Näf, K.; Axelman, J.; Bandh, C.; Pettersen, H.; Johstone, R.; Wallberg, P. Environ. Sci. Technol. 1996, 30, 1238−1241.
(21) Gustaffson, O.; Haghseta, F.; Chan, Ch.; Macfarlane, J.; Gschwend, P. M. Environ. Sci. Technol. 1997, 31, 203−209.
(22) Guftafson,K.; Dickhut, R. Environ. Toxicol. Chem. 1997, 16, 452−461.
(23) Baker, J. E.; Eisenreich, S. J.; Eadie, B. J. Environ. Sci. Technol. 1991, 25, 500−509.
(24) Ko, F.-Ch.; Baker, J. E. Mar. Chem. 1995, 49, 171−188.
(25) Raoux, C.; Bayona, J. M.; Miquel, J. C.; Fowler, S. W.; Teyssie, J.-L.; Albaigés, J. Estuarine Coastal Shelf Sci. In press.
(26) Venkatesan; et al. Geochim. Cosmochim. Acta 1980, 44, 789−802.
(27) Shaw; et al. Estuarine Coastal Shelf Sci. 1985, 21, 131−144.
(28) Seifert, W.; Moldovan, J. M. Geochim. Cosmochim. Acta 1978, 42, 359−375.
(29) Seifert, W.; Moldovan, J. M. Geochim. Cosmochim. Acta 1979, 43, 111−126.
(30) Gough, M. A.; Rowland, S. J. Nature 1990, 344, 648−650.
(31) Wang, Z.; Fingas, M.; Sergy, G. Environ. Sci. Technol. 1994, 28, 1733−1746.
(32) Schwarzenbach, R. P.; Gschwend, P. M.; Imboden, D. M. Environmerntal Organic Chemistry; Wiley & Sons: New York, 1993; pp 255−341.
(33) Simó, R.; Grimalt, J.; Albaigès, J. Environ. Sci. Technol. 1997, 31, 2697−2700.

(34) Brorström-Lunden, E.; Lövblad, G. Atmos. Environ. 1991, 25A, 2251−2257.

(35) Masclet, P.; Mouvier, G.; Nikolau, K. Atmos. Environ. 1986, 20, 439−446.

(36) Wakeham, S. G.; Beier, A. Deep-Sea Res. 1991, 38, S943−S968.

(37) Bayona J. M.; Albaigés, J.; Solanas, A. M.; Parès, R.; Garrigues, P.; Ewald, M. Int. J. Environ. Anal. Chem. 1986, 23, 289−303.

(38) Venkatesan, I. Mar. Chem. 1988, 25, 1−27.

(39) Laflamme, R. E.; Hites, R. A. Geochim. Cosmochim. Acta 1978, 42, 289−303.

(40) Tolosa, I.; Bayona, J. M.; Albaigés, J. Environ. Sci. Technol. 1996, 30, 2495−2503.

Received for review November 10, 1998. Revised manuscript received March 16, 1999. Accepted March 31, 1999.

ES9811647